JOURNAL OF Materials CHEMISTRY

Electrorefining of carbonitrothermic vanadium in a fused salt electrolytic bath

Prabhat Kumar Tripathy,*[a] Jagdish Chander Sehra,[a] Kottarath Naduvil Harindran[b] and Achyut Vasudev Kulkarni[c]

[a]*Materials Processing Division, Bhabha Atomic Research Centre, Trombay, Mumbai, 400 085, India*
[b]*Uranium Extraction Division, Bhabha Atomic Research Centre, Trombay, Mumbai, 400 085, India*
[c]*Analytical Chemistry Division, Bhabha Atomic Research Centre, Trombay, Mumbai, 400 085, India. E-mail: pkt@magnum.barc.ernet.in*

Received 3rd April 2001, Accepted 11th July 2001
First published as an Advance Article on the web 29th August 2001

Electrorefining of impure vanadium was carried out in a fused LiCl–KCl–VCl_2 bath. The impure vanadium, a solid solution of vanadium, nitrogen, carbon and oxygen (V,N,C,O), was prepared by carbonitrothermic reduction of V_2O_5. The major impurities present in (V,N,C,O) were: (wt.%) carbon 1.6, oxygen 1.2 and nitrogen 2.5. The maximum purity, current efficiency and metal yield, after refining, were 99.85, 90 and 86 wt.% respectively. The evaluation and characterization of the electrodeposited vanadium were carried out by chemical analysis, scanning electron microscopy, optical microscopy and hardness measurements.

1. Introduction

Among transition metals, vanadium is one of the most sought-after elements for many high temperature engineering applications. Traditionally, vanadium has been essentially used (i) as an alloying additive in steels and titanium alloys, (ii) in commercial magnets, (iii) in superconducting materials, (iv) in nuclear (self-powered) detectors and (v) as a blanket material for fusion reactors.[1–7] Some of the recent applications of vanadium/vanadium hydride (i) as an alternative electrode material to cadmium (in nickel–cadmium batteries), in the Ni–MH battery, where vanadium is used as an alloying component,[8,9] (ii) as a component of hydrogen storage materials,[10] (iii) as a promising alloying component for magnets[11] and (iv) in the fabrication of hydrogen compressors as well as chemical heat pumps,[12,13] have renewed interest in various methods/processes aimed at preparing high purity vanadium.

The preparation of high purity vanadium is accomplished by a combination of reduction and refining techniques. The reduction is usually carried out by reacting a suitable reductant, such as aluminium, calcium or magnesium, with the oxides and/or halides of vanadium.[14–16] Other methods of production, albeit in smaller quantities, include (i) carbothermic reduction of oxides of vanadium[17] and (ii) plasma arc reduction of a mixture containing vanadium pentoxide and carbon.[18] The metal obtained after reduction is usually impure and hence requires post-reduction refining to achieve enhanced purity levels. Various post-reduction refining techniques which have been applied to vanadium include (i) electron beam melt refining, (ii) the iodide process, (iii) gettering, (iv) fused salt electrolysis, (v) electron beam float zone melting and (vi) solid state electrotransport.[1] From among these techniques, electrorefining of impure vanadium in a fused salt bath has been found to be advantageous for many reasons. Besides being semi-continuous in nature, this process has been found to be (i) quite versatile in refining a wide variety of anode feed materials and (ii) highly effective with respect to the removal of the interstitials as well as a number of commonly associated metallic impurities.[19–21]

In the present investigation, the fused salt electrorefining process was applied for the preparation of high purity vanadium from a low cost vanadium intermediate. This intermediate was prepared by nitriding a mixture of vanadium pentoxide (V_2O_5) and graphite powder to form VN, which was subsequently denitrided to (V,N,C,O) under pyrovacuum conditions. The electrorefining of (V,N,C,O) was carried out in a LiCl–KCl–VCl_2 bath. The effects of various experimental parameters on the extent of refining of (V,N,C,O) have been discussed. The electrodeposited vanadium was evaluated and characterized by chemical analysis, sieve analysis, hardness measurements, optical microscopy and scanning electron microscopy.

Theoretical considerations

Electrorefining of vanadium in the cell

$$V_{(impure)} \mid LiCl–KCl–VCl_2 \mid V_{(pure)}$$

can be represented as[22]

$$\text{Anode: } V_{(impure)} + 2Cl^- \rightarrow VCl_2 + 2e^- \quad (1)$$

$$\text{Cathode: } VCl_2 + 2e^- \rightarrow V_{(pure)} + 2Cl^- \quad (2)$$

$$\text{Net: } V_{(impure)} \rightarrow V_{(pure)} \quad (3)$$

2.1. Role of impurity elements

The behaviour of various impurity elements during electrorefining can be qualitatively discussed by referring to their position in the eutectic LiCl–KCl emf (reduction) series (Table 1).[23] All the metallic impurities, that are present in vanadium, can be divided into two categories. The elements, occupying positions above vanadium in the series are known as more reactive or baser impurities whereas those elements, which occur below vanadium, in the series, are known as less reactive or nobler impurities. Consequently, the baser

Table 1 Electromotive force series of elements in LiCl–KCl (eutectic) electrolytic system at 450 °C

Couple	E^0_M (M→ Molarity scale)	E^0_m (m→ Molality scale)	E^0_x (x→Mol fraction scale)
Li(I)→Li(0)	−3.304	−3.320	−3.410
Mg(II)→Mg(0)	−2.580	−2.580	−2.580
Mn(II)→Mn(0)	−1.849	−1.849	−1.849
Al(III)→Al(0)	−1.762	−1.767	−1.797
Zn(II)→Zn(0)	−1.566	−1.566	−1.566
V(II)→V(0)	−1.533	−1.533	−1.533
Cr(II)→Cr(0)	−1.425	−1.425	−1.425
Fe(II)→Fe(0)	−1.172	−1.172	−1.172
Pb(II)→Pb(0)	−1.101	−1.101	−1.101
Sn(II)→Sn(0)	−1.082	−1.082	−1.082
Co(II)→Co(0)	0.991	0.991	0.991
Ni(II)→Ni(0)	−0.795	−0.795	−0.795
V(III)→V(0)	−0.76	—	—
Mo(III)→Mo(0)	−0.603	−0.608	−0.638
Cu(II)→Cu(0)	−0.448	−0.448	−0.448
Pt(II)→Pt(0)	0.000	0.000	0.000
Cl_2→Cl^-	+0.322	+0.306	+0.216

impurities readily undergo oxidation at the anode and enter into the electrolyte while nobler impurities, because of their unfavourable free energy, get concentrated at the anode. However, the likelihood of codeposition of a baser impurity, along with vanadium, at the cathode can be prevented either by lowering its activity in the anode feed or by carrying out the electrorefining runs at a controlled manner so that its concentration in the electrolyte does not built up beyond a critical value. The non metallic impurities, such as carbon, nitrogen, oxygen and silicon, are usually present as interstitial carbide, nitride, oxide and silicide respectively. Because of their poor solubility in the halide bath, these elements do not take part in the electrolysis and hence remain in the anode mud/sludge. However, it is important to remember that the corresponding emf values (Table 1) give only the relative order in which these elements appear in LiCl–KCl series and do not give any information, whatsoever, about the actual electrode kinetics, during electrolysis, which is solely governed by the over voltage.

3. Experimental

3.1. Materials

3.1.1. Preparation of vanadium nitride. Calculated quantities of V_2O_5 and graphite powder (in the oxide-to-carbon ratio of 1 : 4) were first thoroughly mixed and then pelletized in a 15 mm diameter die. The pellets were then heated in a 30 kW medium frequency laboratory vacuum induction furnace, under continuous nitrogen flow, to a temperature of 1500 °C for a duration of 3 h. The nitride (VN) obtained under optimized conditions, was analyzed as vanadium: 73%; nitrogen: 20.98%; carbon: 3.0% and oxygen: 2.5%.

3.1.2. Thermal decomposition of vanadium nitride. The vanadium nitride thus obtained was thermally decomposed to (V,N,C,O) at a temperature of 1750 °C and under an ultimate vacuum of 0.05 Pa, in the same furnace. Upon chemical analysis, the alloy was found to contain (wt.%) 94.4: vanadium; 2.5: nitrogen; 1.6: carbon; 1.2: oxygen; 0.12: silicon; 0.18: total metallic impurities.

The experimental details pertaining to the preparation of vanadium nitride and its subsequent thermal decomposition to (V,N,C,O) have been discussed elsewhere.[24,25]

3.2. Equipment

The electrorefining cell, with a diameter of 0.15 m, consisted of two chambers: the lower one for containing the electrolyte and anode feed and the upper one, also called the receiver chamber, in which the electrodeposited metal was cooled. Both the chambers were separated by a receiver lock arrangement which, when closed, could isolate the electrolytic cell from coming into contact with the open atmosphere. The receiver chamber had the provision for inserting the chlorinator and cathode and was also equipped with a water cooling arrangement. A high density cylindrical graphite container (0.25 m long, 0.14 m outer diameter and 0.12 m inner diameter) was used for containing the electrolyte and anode feed. A specially designed graphite chlorinator was used to generate the functional electrolyte (VCl_2) *in situ* in the molten salt bath. Fig. 1 shows the schematic diagram of the electrolytic cell and other components.

3.3. Procedure

Calculated quantities of the salt mixture, consisting of GR grade LiCl and KCl, were slowly vacuum dried up to a temperature of 400 °C, until the moisture content became less than 0.01%. The mixture was then melted under a high purity argon atmosphere by gradually raising the temperature to 800 °C. To the molten salt mixture, vanadium dichloride (VCl_2) was added by *in situ* chlorination of vanadium at 750 °C with a mixture of argon and chlorine. The argon and chlorine gas mixture was passed continuously during the reaction at flow rates of 1.66×10^{-6} m^3 s^{-1} and $0.83–1.66 \times 10^{-6}$ m^3 s^{-1} respectively in order to achieve the desired bath composition. The electrolytic bath was pre-electrolyzed with a view to removing the nobler impurities from the electrolyte, using graphite as the cathode, before carrying out the actual refining test runs. The bath was cooled to room temperature after pre-electrolysis, and the anode feed was put in the cell. The electrorefining experiments were carried out under varying experimental conditions, with a view to depositing vanadium on a molybdenum (0.18 m long, 0.025 m wide and 0.001 m thick) cathode. The supply of dc power to the electrolytic cell was provided from a full wave selenium rectifier with variable output.

After completion of each run, the cathode was lifted to the receiver chamber, cooled to room temperature and then taken

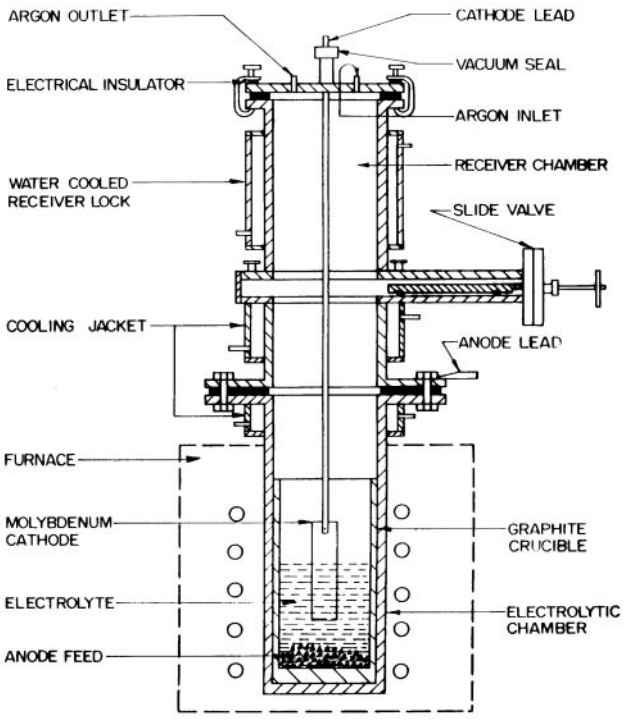

Fig. 1 Inert atmosphere electrolytic cell assembly.

Table 2 Effect of cathode current density on the particle size distribution of the electrodeposited vanadium (temperature: 620 °C, duration: 40 A h)

Cathode current density/A m^{-2}	Mesh size distribution (wt.%)	
	+80 (>840 μm)	−80 (<840 μm)
1076	96.4	03.6
2153	95.8	04.2
3229	93.5	06.5
4305	88.0	12.0
5382	79.6	20.4
6458	66.4	33.6

out of the cell. The vanadium deposits were first repeatedly washed with acidified water (water-to-HCl ratio 20 : 1), then with demineralized water and finally with acetone before carrying out further characterization studies.

4. Results and discussion

The experimental parameters such as (i) cathode current density, (ii) electrolysis temperature and (iii) soluble vanadium content, as VCl_2, in the bath were found to have significant bearing on the quality and quantity of the electrodeposited vanadium.

4.1. Effect of cathode current density (CCD)

Cathode current density (CCD) affects the yield, particle size distribution and purity of the product. The deposition characteristics of electrodeposited vanadium were studied in the CCD range 1076–6458 A m^{-2}. It was observed that a mixture of dendritic and powdery deposits was obtained at all the CCDs. However, the product was predominantly coarser and crystalline at CCDs lower than 3229 A m^{-2}. Similarly, the deposits were more powdery in nature at CCDs higher than 3767 A m^{-2} (Table 2). Because of the powdery nature, these deposits were found to be chemically less pure than the relatively coarser fractions. Best quality deposits were obtained from a narrow CCD range, *i.e.* 2691–3170 A m^{-2}. The optimum CCD was found to be 3170 A m^{-2}.

The effect of CCD on cathode current efficiency (CCE) was also studied. It was observed that the value of CCE was as low as 25% at a CCD of 1076 A m^{-2} (Fig. 2). An increase in the value of CCE was observed with a rise in the applied CCD. The maximum achievable CCE was 90% at a CCD of 4305 A m^{-2}. Further increase in CCD, beyond 4305 A m^{-2}, however, caused a decrease in the apparent CCE. For example, the CCE decreased from a maximum value of 90% to down to 45% when the applied CCD was increased from 4305 A m^{-2} to 6458 A m^{-2}. One of the reasons for such a fall might be due to the formation of more powdered vanadium which resulted in poor adherence to the cathode.

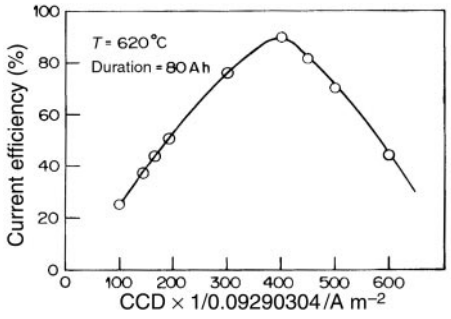

Fig. 2 Effect of cathode current density on cathode current efficiency.

Table 3 Effect of temperature on the particle size distribution of the electrodeposited vanadium (CCD: 3170 A m^{-2}, duration: 40 A h)

Temperature/°C	Mesh size distribution (wt.%)	
	+80 (>840 μm)	−80 (<840 μm)
550	75.2	24.8
580	80.4	19.6
600	93.5	06.5
620	94.8	05.2
640	88.3	11.7
660	77.0	23.0
680	65.3	34.7

4.2. Effect of temperature

Like CCD, electrolysis temperature also affects both CCE as well as the size of the electrodeposit. At lower temperatures, *i.e.* near the melting point of the bath, fluidity and electrical conductivity are generally poor. Metals deposited at low temperatures are fine grained and adhere poorly to the cathode resulting in lower current efficiency.[26] Also at lower temperatures, the electrolyte drag-out becomes higher. On the other hand, an increase in the bath temperature favours enhanced diffusion and reaction rates, thereby resulting in higher mass transfers. Higher temperatures also increase the bath conductivity and fluidity. Increased electrolysis temperature promotes the rate of crystal growth with better adhesion to the cathode.

It was observed that within the temperature region 600–620 °C the cathode deposit was coarser in nature. The percentage of the coarser fraction started decreasing at temperatures less than 600 °C and above 620 °C (Table 3). At temperatures less than 580 °C, the metal yield was poor and the product was powdery. Also, the salt drag-out which surrounded the cathode deposit was found to be higher at lower temperatures. At temperatures higher than 650 °C, the deposits were more powdery in nature. The optimum temperature of electrolysis was found to be 620 °C.

The bath temperature was also found to influence the CCE. Initially, the CCE increased with increasing temperature, reached a peak value and finally showed a downward slide (Fig. 3). The maximum value of CCE was obtained at 620 °C. The decrease in apparent CCE at higher temperatures was due to the formation of a predominantly powdery vanadium deposit which eventually fell into the bath. This was verified by observation of a very fine vanadium powder which was trapped in the electrolyte.

4.3. Effect of time

As expected, the quantity of vanadium was found to increase with electrolysis time during the initial stages of electrolysis when the percentage of anode feed electrolyzed was relatively low. Fig. 4 shows the percentage increase in CCE with electrolysis time for a typical test run, conducted at 620 °C under a CCD of 3170 A m^{-2}.

However, upon prolonged electrolysis, as the quantity of

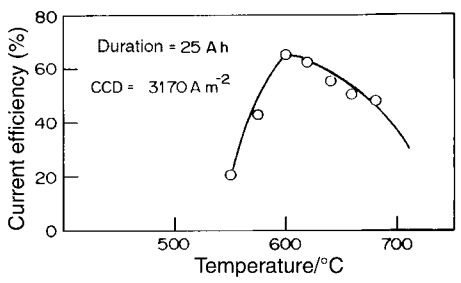

Fig. 3 Effect of temperature on cathode current efficiency.

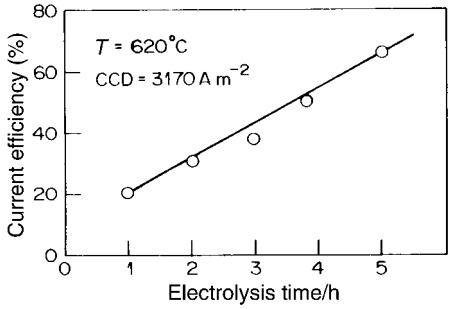

Fig. 4 Increase in current efficiency with electrolysis time.

vanadium in the anode feed went on decreasing, a simultaneous decline in the quantity of vanadium deposited at the cathode was also observed. In addition to this prolonged electrolysis, not adding fresh anode feed when the vanadium content in the anode feed decreased substantially was found to render increasingly powdery deposits (Table 4). Besides being fine in nature, these deposits were found to be relatively less pure.

4.4. Effect of soluble vanadium content in the bath

The soluble vanadium content in the electrolyte, in the form of VCl_2, affected both the yield and quality of vanadium deposited on the cathode. It was observed that a minimum of 3.0 wt.% vanadium was necessary to obtain good quality vanadium crystals. As the vanadium concentration was progressively increased to 6.7%, the deposited vanadium crystals became coarser and more adherent in nature raising the overall CCE to a maximum value of 90%. There was no further improvement in CCE upon further raising the soluble vanadium concentration to 9.0%. As a result of this finding, we chose to maintain an optimum soluble vanadium concentration at 6.7% which corresponded to 16% VCl_2. Accordingly, all our investigations were subsequently carried out in a bath comprising 37 wt.% LiCl, 47 wt.% KCl and 16 wt.% VCl_2.

4.5. Chemical purity of the electrodeposited vanadium

The purity of the electrodeposited vanadium was found to depend on several factors such as (i) current density, (ii) temperature, (iii) electrolysis duration, (iv) quality and (v) quantity of the anode feed. In general, very high current density as well as temperature yielded relatively finer vanadium deposits, which were also found to be chemically less pure, whereas vanadium obtained under optimum conditions was found to have relatively better purity. Also, prolonged electrolysis, without adding fresh anode feed periodically, resulted in the deposition of relatively less pure vanadium metal.

The chemical purity was also found to vary between different size fractions. The coarser crystals were found to be purer than the powdered/more fine vanadium deposits. Crystals having sizes $\geqslant$840 μm were found to be the purest ones. Effective purification in these size fractions with respect to zinc, cobalt, manganese, magnesium and calcium could be achieved when

Table 4 Change in the average particle size of the electrodeposited vanadium with respect to the decreased vanadium content in the anode feed

Cumulative vanadium recovery from the anode feed (wt.%)	Average particle size (wt.%)	
	+80 mesh (840–177 μm)	−80 mesh (149–74 μm)
Up to 39	86	14
Between 41–50	77	23
Between 53–72	68	32
Between 78–89	58	42

Table 5 Chemical analysis of the electrodeposited vanadium obtained at 3170 A m^{-2} and 620 °C

Impurity element	Amount (ppm)
Aluminium	21
Calcium	1.2
Carbon	660
Chromium	74
Cobalt	0.4
Iron	114
Magnesium	0.4
Manganese	0.6
Molybdenum	ND
Nickel	27
Nitrogen	4
Oxygen	500
Silicon	50
Zinc	0.4
Vanadium (wt.%)	99.85

ND→Not Detected.

the concentration of these impurities was less than 55 ppm. Most of the vanadium samples in theses size ranges contained zinc, molybdenum and calcium below detectable limits, whereas the concentrations of copper, aluminium, lead, sodium and iron were found to be as low as 7, 21, 68, 76 and 114 ppm respectively. Other size fractions ($\leqslant$149 μm) were found to contain significant amounts of iron (in the range 0.1–0.8%), chromium (in the range 0.1–0.6%) and nickel (in the range 0.1–0.3%). Among non-metallic impurities, nitrogen could be lowered to an extremely low level. In all the refined vanadium samples (of sizes $\geqslant$840 μm), nitrogen, oxygen and carbon concentrations were found in the ranges 4–60, 200–1000 and 660–1700 ppm respectively. However, in other vanadium samples (where the crystallite sizes were less than 149 μm), values of nitrogen and oxygen were found to be significantly higher, *i.e.* in the ranges 400–1000 and 2000–4000 ppm, whereas carbon contents were marginally higher (1800–2000 ppm). The chemical analysis of one of the best deposits is given in Table 5. The overall purity and recovery of vanadium samples obtained under different experimental conditions were in the ranges 98.5–99.8% and 86% respectively.

According to Rostoker, ductile vanadium must contain less than about 0.2 wt.% oxygen and nitrogen together whereas carbon in amounts of less than 0.25 wt.% does not increase the hardness of the metal.[27] In his book, Simons has mentioned that the limits of chemical composition (maxima) for vanadium are: Fe: 0.05%; C: 0.95%; N: 0.05%; H: 0.01%; O: 0.09%. If these limits are exceeded, particularly for oxygen, nitrogen, hydrogen and carbon, the mechanical properties of vanadium will suffer.[28] Yet in another paper, Bose has mentioned that the combined value of nitrogen, carbon and oxygen must be less than 0.25 wt.% for vanadium to be ductile.[29] The chemical analysis of the vanadium metal obtained by the present process has shown a significant reduction in the total impurity content, *i.e.* from an initial value of 5.6% to a value down to just 1500 ppm, and thus amply demonstrates the efficacy of the present process.

5. Characterization of electrodeposited vanadium crystals

The electrodeposited vanadium was characterized with respect to particle size distribution and hardness measurements. The distribution of impurity elements and growth morphology of the vanadium crystals during electrodeposition were studied under optical and scanning electron microscopes respectively.

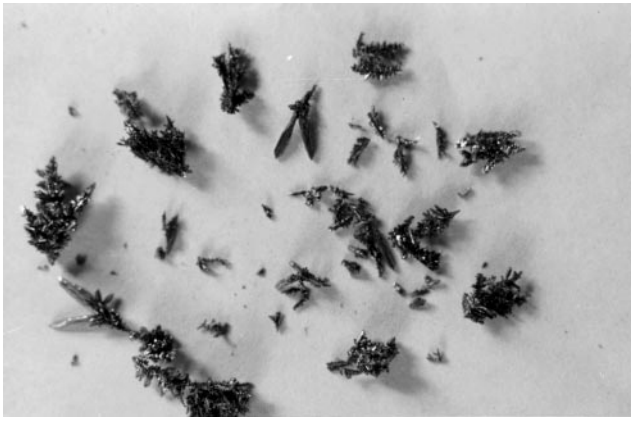

Fig. 5 Coarse and crystalline vanadium fraction ($\geqslant$840 μm).

5.1. Particle size distribution

The electrodeposited vanadium crystals were sieved into different mesh sizes with a sieve shaker. The +20 fraction consisted of mostly dendritic/coarse vanadium crystals (Fig. 5) whereas the fractions between −20 to +35, −35 to +45, −45 to +60, −60 to +80 consisted of a mixture of fine needle-like/dendritic crystals and coarse powder. The −80 fraction was mostly finely powdered vanadium. Table 6 describes the particle size distribution of the electrodeposited vanadium.

5.2. Hardness measurement

The electrodeposited vanadium crystals (of size +20 mesh or $\geqslant$840 μm) were first pelletized and then consolidated into buttons in an arc (non-consumable) melting furnace. One side of these buttons was polished to a smooth surface before determining the hardness. The measurement was done in an EMCO autohardness tester machine and was found to be in the range 50–60 VHN (Vicker's Hardness Number).

5.3. Optical microphotograph

The arc melted vanadium buttons were mounted on araldite moulds and then polished on 110, 220, 400 and 600 grit emery papers. The buttons were finally polished on a diamond wheel. The samples were then viewed through an optical microscope under a magnification of 300×. The photographs of unetched samples showed almost identical features. A typical microphotograph is shown in Fig. 6, which revealed the existence of a single phase system. The dispersion of fine structures may be due to the presence of (i) defects and/or (ii) impurities. The needle shaped and more fine structures and somewhat blunt shaped/spherical structures probably represent the defects and impurity elements respectively. The appearance of parallel lines seen in the photograph is perhaps due to the presence of scratches along the polishing direction. However, as the micrographic samples were prepared with utmost care, the presence of these lines may be due to the inherent ductility of the metal.

Table 6 Particle size distribution of the electrodeposited vanadium

Mesh size	Percentage (average)	Size range/μm	% +80 mesh fraction (cumulative)	% −80 mesh fraction (cumulative)
+20	22.00	$\geqslant$840		
−20+35	20.56	840–500		
−35+45	11.43	500–350		
−45+60	12.67	350–250		
−60+80	11.26	250–177		
−80+100	4.43	177–149	77.92	22.08
−100+120	5.06	149–125		
−120+140	2.84	125–105		
−140+200	5.63	105–74		
−200	4.12	<74		

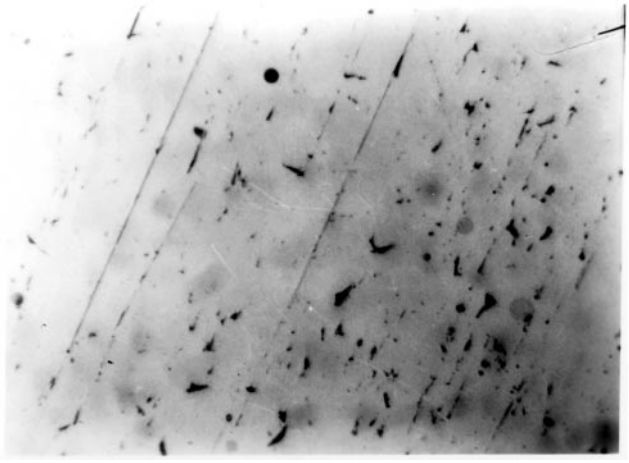

Fig. 6 Optical microphotograph of arc melted vanadium button (unetched).

5.4. SEM photograph

The SEM photographs of vanadium crystals were recorded in a JEOL scanning electron microscope under different magnifications. All the photographs clearly showed the dendritic growth features of the vanadium crystals. It was observed that the applied cathode current density influenced the growth morphology of these crystals. The metal obtained at a CCD of 2325 A m^{-2} showed maximum dendritic features comprising primary, secondary, tertiary and quaternary growth patterns (Fig. 7). At both lower and higher CCD values than 2325 A m^{-2}, the dendritic growth appeared to be suppressed. In some other samples, a typical pyramid structure was seen (Fig. 8). The formation of this structure indicated that the tip of the pyramid was the direction of the growth of columnar crystals.

6. Conclusion

The present investigation has shown the feasibility of the transformation of vanadium nitride to high purity vanadium metal in a LiCl–KCl–VCl_2 bath. Besides being a low cost material, the anode feed employed in the present investigation was found to be attractive from the point of view of the

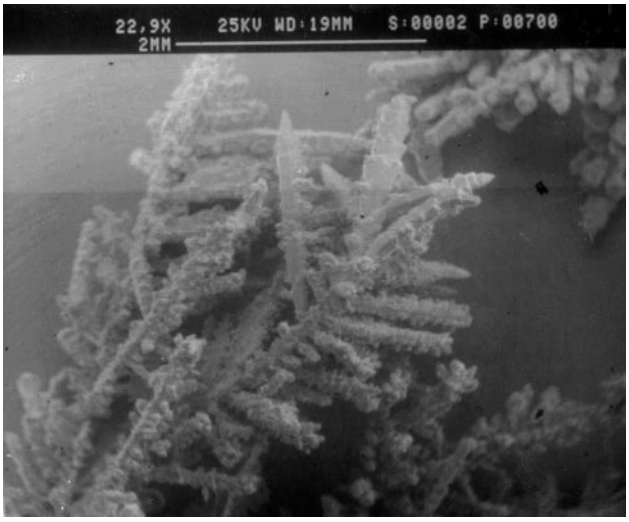

Fig. 7 Scanning electron microphotograph of vanadium crystal, obtained at a cathode current density of 2325 A m^{-2}.

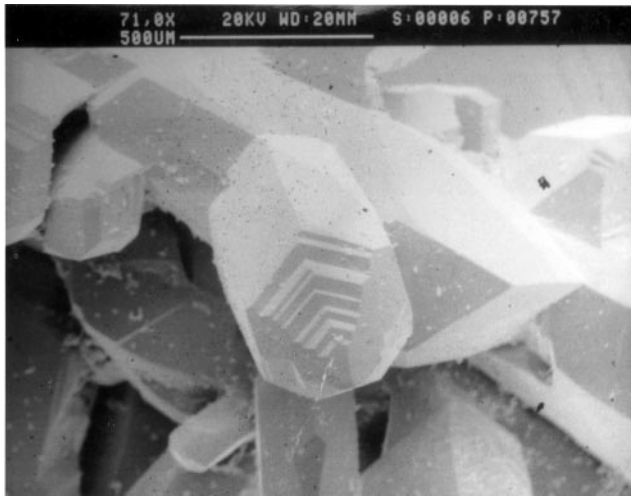

Fig. 8 Typical pyramid structure of vanadium crystal, obtained at a cathode current density of 3170 A m^{-2}.

achievable purity of vanadium metal as well as its overall recovery.

References

1 C. K. Gupta and N. Krishnamurthy, in *Extractive Metallurgy of Vanadium*, Elsevier, Amsterdam, The Netherlands, 1992.
2 R. I. Jaffee, *An overview of titanium development and applications*, in *Titanium-80, Science and Technology*, ed. H. Kimura and O. Izumi, vol. 1, The Metallurgical Society of AIME, Warrendale, PA, 1980, pp. 53–74.
3 G. F. Hardy and J. K. Hulm, *Phys. Rev.*, 1954, **93**, 1004.
4 D. Hughes, *Superconductors - Practical Aspects*, in *Encyclopedia of Materials Science and Engineering*, ed. M. B. Bever, Pergamon, NY, 1986, pp. 1771–1778.
5 Y. Israel and L. Meites, in *Encyclopedia of Chemistry of the Elements*, vol. 7, ed. A. J. Bard, Marcel Dekker, NY, 1976, pp. 418–450.
6 C. T. Liu, *J. Nucl. Mater.*, 1979, **85–86**, 907.
7 J. Bethin and A. Tobin, *J. Nucl. Mater.*, 1984, **122 & 123**, 864.
8 X. G. Yang, Q. A. Zhang, K. Y. Shu, Y. Q. Lei, Q. D. Wang and W. K. Zhang, *J. Alloys Compds.*, 1999, **287**, 104.
9 M. Tsukahara, K. Takahashi, A. Isomura and T. Sakai, *J. Alloys Compds.*, 1999, **287**, 215.
10 D. M. Kim, H. Lee, K. J. Jang and Y. J. Lee, *J. Electrochem. Soc.*, 1998, **145**, 3387.
11 Z. Liping, Z. Kaiwen, W. Shiwei and Z. Yinghong, *J. Alloys Compds.*, 1999, **287**, 195.
12 J. J. Reilly and R. H. Wiswall, *Inorg. Chem.*, 1970, **9**, 1678.
13 G. G. Libowitz and A. J. Mealand, *J. Less Common Met.*, 1987, **131**, 275.
14 R. K. McKechnie and A. U. Seybolt, *J. Electrochem. Soc.*, 1950, **97**, 311.
15 O. N. Carlson, F. A. Schmidt and W. E. Krupp, *J. Met.*, 1966, **18**, 320.
16 T. T. Campbell, J. L. Schaller and F. E. Block, *Metall. Trans.*, 1973, **4**, 237.
17 K. Ono and J. Moriyama, *J. Less Common Met.*, 1981, **81**, 79.
18 K. Mimura, W. L. Gu and K. Tiniuchi, *J. Mining Met. Inst. Jpn.*, 1982, **98**, 43.
19 T. A. Sullivan, *J. Met.*, 1965, 45.
20 K. P. V. Lei and T. A. Sullivan, *Metall. Trans.*, 1971, **2**, 2312.
21 K. P. V. Lei, F. R. Cattoir and T. A. Sullivan, Report of Investigation No.-6972, US Bureau of Mines, Washington DC, 1967.
22 T. K. Mukherji and C. K. Gupta, *Trans. Soc. Electrochem. Sci. Technol.*, 1976, **11**, 126.
23 J. A. Plambeck, *J. Chem. Eng. Data*, 1967, **12**, 77.
24 P. K. Tripathy, J. C. Sehra and A. V. Kulkarni, *J. Mater. Chem.*, 2001, **11**, 691.
25 P. K. Tripathy, *J. Mater. Chem.*, 2001, **11**, 1514.
26 V. G. Gopienko, *Electrorefining of titanium in titanium and titanium alloys*, ed. J. C. William and A. F. Belof, Plenum Press, NY, 1982, p. 117.
27 W. Rostoker, *The metallurgy of vanadium*, John Wiley & Sons, NY, 1958, p. 68.
28 E. N. Simons, *Guide to uncommon metals*, Frederick Muller Ltd., Fleet Street, London, 1967, p. 226.
29 D. K. Bose, *Miner. Proc. Extr. Metall. Rev.*, 1992, **10**, 217.